MEDICAL SCIENCE MONITOR

CLINICAL RESEARCH

e-ISSN 1643-3750
© Med Sci Monit, 2020; 26: e923541
DOI: 10.12659/MSM.923541

Received: 2020.02.16
Accepted: 2020.04.02
Available online: 2020.04.21
Published: 2020.06.11

A Novel Metallic Artifact Reduction Technique When Using a Computed Tomography-Guided Percutaneous Metallic Antenna to Ablate Malignant Pulmonary Nodules: A Qualitative and Quantitative Assessment

Authors' Contribution:
Study Design A
Data Collection B
Statistical Analysis C
Data Interpretation D
Manuscript Preparation E
Literature Search F
Funds Collection G

BCF Guorong Wang
ADE Zhiwei Wang
AF Zhengyu Jin

Department of Radiology, Peking Union Medical College Hospital, Beijing, P.R. China

Corresponding Author: Zhiwei Wang, e-mail: zhiweiwang1981@sina.com
Source of support: This study was funded by National Public Welfare Basic Scientific Research Program of Chinese Academy of Medical Sciences (grant numbers 2018PT32003 and 2017PT32004)

Background: Metallic microwave ablation (MWA) antenna-related artifacts are usually created in conventional CT images, and these artifacts can influence the effect of ablation. The aim of this study was to evaluate a new type of metal artifact reduction (MAR+) technique in CT-guided MWA for lung cancer.

Material/Methods: This retrospective study enrolled 30 lung cancer patients who received CT-guided MWA treatment from December 2017 to April 2018. Images after microwave antenna insertion into the tumor were reconstructed by the filter back projection (group A) and MAR+ reconstruction (group B). The CT values and standard deviations of the regions of interest (ROIs) on the chosen image were recorded, including the most significantly hypodense artifact (ROI_1), hyperdense artifacts (ROI_2), and chest muscles of the same layer (ROI_3). The metal artifact indexes based on ROI_1 and ROI_2 (AI_1, AI_2) and the overall metal artifact index (AI) were calculated. Subjective image quality was graded on a five-point scale (1=worst, 5=excellent).

Results: The AI_1 (74.14±76.32), AI_2 (13.75±19.02) and AI (54.12±54.82) of group B were lower than those of group A [(153.33±89.04), (30.63±26.42), (112.00±63.10), respectively] ($P<0.001$ for all). Both radiologists reported that the subjective image value of group B was significantly higher than that of group A ($P<0.001$). The subjective image quality scores evaluated by 2 observers showed excellent consistency (ICC=0.829).

Conclusions: The MAR+ imaging reconstruction significantly reduced metal artifacts, which helps radiologists to clearly observe the relationship between the ablation antenna and the lesion.

MeSH Keywords: Artifacts • Lung Neoplasms • Microwaves • Tomography, X-Ray Computed

Full-text PDF: https://www.medscimonit.com/abstract/index/idArt/923541

2119 3 2 33

Indexed in: [Current Contents/Clinical Medicine] [SCI Expanded] [ISI Alerting System] [ISI Journals Master List] [Index Medicus/MEDLINE] [EMBASE/Excerpta Medica] [Chemical Abstracts/CAS]

Background

Lung cancer is the most commonly diagnosed cancer (11.6% of all cancers) and the most common cause of cancer death (18.4% of all cancer deaths) worldwide [1]. In recent years, percutaneous microwave ablation (MWA), as a novel local treatment modality, has been widely used for lung cancer therapy [2–4]. MWA uses electromagnetic waves in the microwave energy spectrum to generate tissue-heating effects. The current MWA manufacturer uses a frequency of 2450 MHz. The polar molecules such as water molecules in tumor tissue generate extremely high-speed vibrations under the action of this microwave electromagnetic field, causing collisions and friction between molecules, and the thermal energy is then transferred to the adjacent tissues. When the temperature reaches 60~150°C in a short time, it causes irreversible damage to cells or coagulative necrosis [5,6]. Moreover, a single MWA probe covered a larger ablation volume than radiofrequency ablation (RFA) [7]. Computed tomography (CT) is currently the most accurate image-guidance technique for lung ablation.

The efficiency of MWA depends on the appropriate and accurate location of the microwave ablation antenna in the tumor. However, metal instruments used in interventional procedures can create significant artifacts in CT images [8]. The severity of metal artifacts depends on the material of the instruments used. MWA antenna-related artifacts are usually created in conventional CT images. Severe artifacts can cover the surrounding tissues and influence the exact location of the ablation antenna [9,10]. Therefore, reducing artifacts is very important for MWA.

To reduce these artifacts, the optimal acquisition and reconstruction method must be used for patients with various types of metal prostheses and implants. However, metal artifact reduction (MAR) techniques are rarely applied in interventional therapy. The aim of this study was to evaluate a new type of metal artifact reduction (MAR+) technique in CT-guided MWA for lung cancer.

Material and Methods

This retrospective study was approved by the Institutional Review Board of our hospital. The requirement for informed consent was waived for all subjects. We retrospectively reviewed patients with lung cancer who underwent CT-guided MWA using the MAR+ technique between December 2017 and April 2018. A total of 30 patients were identified.

CT-guided MWA procedure

All ablation processes for lung cancer were performed with the guidance of a NeuViz 128 CT (Neusoft Medical Company, Shenyang, China). The scanning parameters for the location were 120 kVp tube voltage, automatically modulated tube current (reference mAs: 180), 0.6 second gantry rotation time, 1.2 pitch, 128×0.625 mm collimation width, 360 mm field of view (FOV), 5 mm slice thickness, and 5 mm slice intervals. The effective dose-length product (DLP, mGy×cm) was recorded, and the effective dose (ED, mSv) was calculated for each ablation series using the equation: ED=DLP×k [k=0.014 ($mSv \times mGy^{-1} \times cm^{-1}$)]

Patients underwent a CT scan of the area of interest during suspended inspiration. The entry site was prepared and draped in a sterile fashion. All ablations were performed under local anesthesia consisting of an injection of 5–10 mL of 1% lidocaine hydrochloride. All ablations were performed by a microwave ablation system (2450 MHz generator, MICRO TECH, KANG YOU, Nanjing, China) and a 16-gauge antenna (made of stainless steel as biomedical material). The antenna was inserted into the lesion during a breath-hold. Five-millimeters sections with image reconstruction were then obtained during the breath-hold to verify the location of the antenna (Figure 1A–1D). The ablation power and time were adjusted to the size and location of the tumor according to the manufacturer's recommendations. All ablations were performed at a constant power of 50–60 W. The ablation time per tumor was 5–10 minutes. The procedure aimed to ablate the tumor plus at least a 5-mm margin.

After the ablation procedure, CT images were immediately acquired at the level of the ablation site to search for the presence of complications, such as pneumothorax or parenchymal hemorrhage.

Image postprocessing

The raw data of all available images after microwave antenna insertion into the tumor site were reconstructed by the filter back projection algorithm (group A) and MAR+ reconstruction (group B). The reconstruction parameters of group A and B were: group A with Clearview closed, MAR+ closed; group B with Clearview 40%, MAR+ open. Both groups were reconstructed with a slice thickness of 5 mm and a slice interval of 5 mm. Actual MWA procedures were performed under the guidance of group B images. The images of groups A and B were transferred to the advanced workstation (AVW 1.0.8, Neusoft Medical Company, Shenyang, China) for further analysis.

MAR+ technique is a kind of normalized MAR, which involves a special method to reduce the effect of the microwave antenna. The MAR+ algorithm was created in the following way: according to the geometric parameters of the system, the characteristics of the electronic components and the detector, the anatomical model, the front projection model, and the noise model are refined. The correction process based on the iterative algorithm

Indexed in: [Current Contents/Clinical Medicine] [SCI Expanded] [ISI Alerting System] [ISI Journals Master List] [Index Medicus/MEDLINE] [EMBASE/Excerpta Medica] [Chemical Abstracts/CAS]

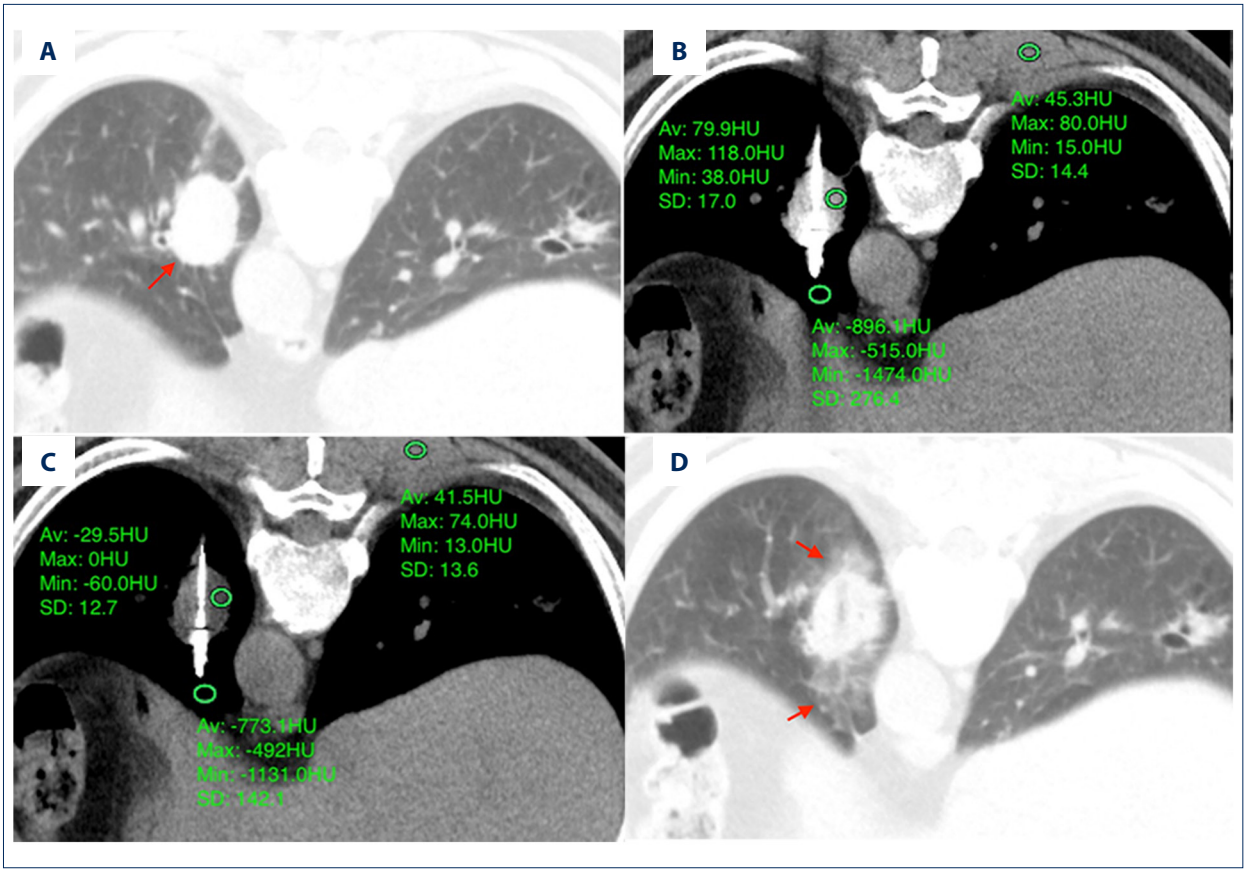

Figure 1. A 58-year-old man with the primary lung cancer who underwent MWA treatment. (**A**) An axial plain CT image before the ablation process showing an elliptical nodule of 3.4×2.4 cm in the basal right lower lobe in the lung window (red arrow). (**B**) The axial plain CT scan after filter back projection reconstruction presenting with poor quality, where the extensive metal artifacts impair the assessment of the antenna's position within the nodule. (**C**) The axial plain CT scan after MAR+ reconstruction appearing with excellent quality where the metal artifacts are greatly reduced, allowing better visualization of the relationship of the antenna and lesion. (**D**) An axial plain CT scan after the biopsy procedure showing patchy areas of ground-glass opacity around the lesion (red arrows).

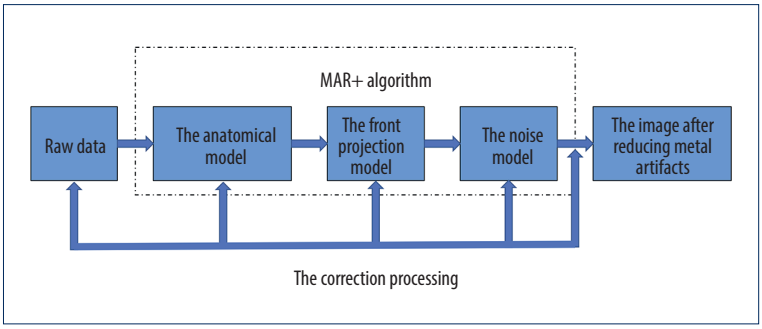

Figure 2. The flow of the MAR+ technique.

removes the noise caused by metal and restores the true anatomical structure around the metal object (Figure 2).

Evaluation methods

The images that included the tip of the microwave antenna and the lesion with the most severe artifacts were chosen for analysis by 2 radiologists (with 5 and 8 years of experience in chest imaging) independently in the soft-tissue window (window width: 300 HU, window level: 40 HU). Any disagreements were resolved by discussion and consensus.

Indexed in: [Current Contents/Clinical Medicine] [SCI Expanded] [ISI Alerting System] [ISI Journals Master List] [Index Medicus/MEDLINE] [EMBASE/Excerpta Medica] [Chemical Abstracts/CAS]

Subjective evaluation

Two radiologists, who were blinded to the imaging reconstruction method, graded on a five-point scale [11] in each patient based on an overall assessment of the severity of metal artifacts. The images were evaluated for subjective evaluation in the soft-tissue window setting (window width: 300 HU, window level: 40 HU). The specific standards were: 1-worst, severe metal-related artifacts that hardly reveals the surrounding lung cancer tissue; 2-bad, limited observation of the surrounding tissue; 3-medium, some artifact but acceptable visualization; 4-good, small enough artifact to clearly observe the relationship between the microwave antenna and the lesion; 5-excellent, almost no artifact.

Objective evaluation

The objective evaluation was performed by another radiologist with 3 years of experience in chest imaging in the soft-tissue window (window width: 300 HU, window level: 40 HU). The CT values in Hounsfield units (CT_1, CT_2, CT_3) and standard deviations (SD_1, SD_2, SD_3) of the elliptical regions of interest (ROIs) with the area of 30–40 mm^2 were recorded, including the most significantly hypodense artifacts (ROI_1) and hyperdense artifacts (ROI_2) of the selected image, along with chest muscles (ROI_3) of the same slice. The metal artifact indexes based on ROI_1 and ROI_2 (AI_1, AI_2) and the overall metal artifact index (AI) were calculated as shown below [12,13], respectively.

$$AI_1=\sqrt{SD_1^2-SD_3^2},\ AI_2=\sqrt{SD_2^2-SD_3^2},\ AI=\sqrt{(AI_1^2+AI_2^2)/2}$$

Statistical analysis

Statistical analysis was performed with SPSS (version 20.0, SPSS Inc., Chicago, USA). The discrete variables are expressed as median and interquartile range, and the continuous variables are expressed as mean±SD. A paired *t* test was used to compare the differences in AI_1, AI_2, and AI between the 2 groups. The subjective scores were compared using a Wilcoxon signed-rank test. The consistency between the 2 readers was evaluated by the intraclass correlation coefficient (ICC) test with the following scale: poor (<0.40), moderate (0.40–0.60), good (0.60–0.75), and excellent (>0.75) [14]. P<0.05 was considered statistically significant.

Results

General characteristics

The general patient characteristics are summarized in Table 1. All 30 lung cancer patients underwent MWA therapy for a single lesion. Twenty-one cases (70%) were primary pulmonary cancers (adenocarcinoma, n=16; squamous cell carcinoma, n=5), and 9 cases were metastatic cancers (esophageal squamous cell carcinoma, n=1; hepatocellular carcinoma, n=3; colorectal adenocarcinoma, n=5). There were 7 women (23.3%) and 23 men (76.7%) with a mean age of (60.3±11.6) years (range 38–77 years). The median tumor size was (3.5±0.7) cm (range 2.3–4.9 cm). One MWA antenna was used for each patient during the ablation procedure. The mean ED was (2.74±0.43) mSv (range 2.23–3.17 mSv) per scan. The reconstructions utilizing MAR+ algorithms were processed in an average time of (3.2±0.4) seconds.

Table 1. Clinical characteristics of the patients.

Characteristics	Values
Age (years)*	60.3±11.6 (38–77)
Sex	
Male	23 (76.7%)
Female	7 (23.3%)
Histopathological types	
Primary lung cancer	21 (70%)
Adenocarcinoma	15 (71.4%)
Squamous cell carcinoma	6 (28.6%)
Metastatic lung cancer	9 (30%)
Esophageal squamous cell cancer	1 (11.1%)
Hepatocellular carcinoma	5 (55.6%)
Colorectal adenocarcinoma	3 (33.3%)
Tumor size (cm)*	3.5±0.7 (2.3–4.9)
Complications	
Pneumothorax	4 (13.3%)
Pleural effusion	2 (6.7%)
Effective dose (mSv)*	2.74±0.43 (2.23–3.17)

* Data are the mean±standard deviation, and data in parentheses are the ranges or percentages.

Table 2. The values of AI_1, AI_2 and AI were significantly different between groups A and B.

	Group A	Group B	P values
AI_1	153.33±89.04	74.14±76.32	<0.001
AI_2	30.63±26.42	13.75±19.02	<0.001
AI	112.00±63.10	54.12±54.82	<0.001

Data are presented as the mean±standard deviation, and P<0.05 indicates statistical significance.

Indexed in: [Current Contents/Clinical Medicine] [SCI Expanded] [ISI Alerting System] [ISI Journals Master List] [Index Medicus/MEDLINE] [EMBASE/Excerpta Medica] [Chemical Abstracts/CAS]

Table 3. Subjective image quality assessment between groups A and B by 2 radiologists.

Radiologists	Patients	Score 1	Score 2	Score 3	Score 4	Score 5	Mean score*	P value
Radiologist 1								
Group 1	30	20 (66.7%)	10 (33.3%)	0 (0%)	0 (0%)	0 (0%)	1 (1, 2)	P<0.001
Group 2	30	0 (0%)	0 (0%)	5 (16.7%)	15 (50%)	10 (33.3%)	4 (4, 5)	
Radiologist 2								
Group 1	30	20 (66.7%)	10 (33.3%)	0 (0%)	0 (0%)	0 (0%)	1 (1, 2)	P<0.001
Group 2	30	0 (0%)	0 (0%)	4 (13.3%)	18 (60%)	8 (26.7%)	4 (4, 5)	

* Data are the median and interquartile range and data in parentheses are the percentages.

Objective evaluation results

The objective evaluation results are summarized in Table 2. The AI_1, AI_2, and AI of group B (74.14±76.32, 13.75±19.02, 54.12±54.82) were significantly lower than those of group A (153.33±89.04, 30.63±26.42, 112.00±63.10, all P<0.001).

Subjective evaluation results

Radiologist 1 evaluated that the subjective image value of group B was higher than that of group A, and the difference was statistically significant [4 (4, 5) *vs.* 1 (1, 2), P<0.001], which was consistent with the subjective assessment results of Radiologist 2. The subjective image quality scores evaluated by 2 observers showed excellent consistency (ICC=0.829) (Table 3, Figure 1A–1D).

MWA-related results

The technical success rate of MWA treatment for the 30 patients was 100%. The main complications were pneumothorax in 4 patients (13.3%) and pleural effusion in 2 patients (6.7%). No deaths were observed during the ablation process.

Follow-up contrast-enhanced chest CT examinations were used to detect local recurrence. No patients had local recurrence at the ablation site during the short follow-up period (3–6 months).

Discussion

Surgical lobectomy is viewed as the criterion standard treatment for lung cancer [15–17]. However, patients with high-risk conditions, such as cardiopulmonary dysfunction, impaired renal function, and hypertension, or who are elderly, are not good candidates for surgery. Currently, MWA has been widely used in patients with medically inoperable tumors [18]. Several studies have suggested that MWA is safe and effective in the treatment of primary pulmonary malignances and pulmonary metastases [6,16,19,20]. The presence of metallic objects in the imaging field may deteriorate the image quality of CT scans and thus impact treatment [21]. The significance of reducing metallic artifacts is to allow the operator to clearly observe the location of the lesion and the ablation antenna, thus improving the image quality and providing more possibilities for accurate MWA procedures.

The causes of metal artifacts are complex and include beam hardening, photon starvation, and increased scatter and noise [22–24]. To reduce these artifacts, the optimal acquisition and reconstruction method must be used for patients with various types of metal prostheses and implants. Different CT venders have their own specific MAR algorithms. For example, gemstone spectral (GSI) dual-energy CT (DECT) with or without metal artifact reduction software (MARs) from GE (GE Healthcare, USA) used projection-based reconstructions on 40–140 keV monochromatic images to reduce artifacts [24]. Iterative metal artifact reduction (IMAR) algorithms from Siemens (Siemens Healthcare, Germany) used an iterative frequency split technique to suppress metal-related artifacts [25]. Orthopedic metal artifact reduction algorithms (O-MAR) used the iterative reconstruction method developed by Philips (Philips Medical Systems, The Netherlands) [26,27]. Toshiba (Toshiba Medical Systems, Japan) developed the single-energy metal artifact reduction (SEMAR) procedure, which mainly removes the metal artifacts based on a linear interpolation in the blended sinogram (original sinogram and tissue-classified sinogram) [28]. NeuViz 128 CT is configured with the MAR+ technique to clearly remove the metal artifact in a reasonable time, to a certain extent, in case of the presence of complications. The procedure is carried out by creating a front projection model, an anatomy model, and a noise model according to the geometric parameters, electronic components, and detector characteristics, and then clearly removing the metal artifact based on the iterative correction method.

Metal artifact reduction techniques have been applied to evaluate the image visualization of patients with knee

Indexed in: [Current Contents/Clinical Medicine] [SCI Expanded] [ISI Alerting System] [ISI Journals Master List] [Index Medicus/MEDLINE] [EMBASE/Excerpta Medica] [Chemical Abstracts/CAS]

replacements [29], total or unilateral hip arthroplasty [30,31], dental implants [32], and spine metallic implants [33]. Few studies have explored how to decrease the artifacts produced by metallic ablation antennas during CT-guided MWA for patients with lung cancer. In our study, the results showed that MAR+ imaging reconstruction could reduce the MWA antenna-related metal artifacts subjectively and objectively. In images reconstructed with the MAR+ technique, the microwave ablation antenna was observed with a clearer delineation and the removal of metal artifacts at the needle edges. The removal of metal artifacts and the visualization of the soft-tissue region surrounding the antenna were critical, as they can enhance needle confirmation within the target lesion. Although switching to the bone window may partially reduce metal artifacts, the surrounding soft-tissue region is unclear. The MAR+ technique in the present study reduced metal artifacts in only approximately 3 seconds per scan, which is nearly a real-time correction of metal artifacts.

The limitations of this study include its retrospective nature and its fairly small sample size of 30 patients, which limits the generalization of the findings. This study mainly focused on image quality, and the follow-up time was relatively short. The survival and outcomes of the patients require further, long-term, follow-up.

Conclusions

In conclusion, the MAR+ imaging reconstruction algorithm from NeuViz 128 CT significantly reduced metal artifacts, which makes it possible for radiologists to clearly observe the relationship between the ablation antenna and the lesion and thus improves the efficiency and accuracy of MWA procedures.

Conflicts of interest

None.

References:

1. Bray F, Ferlay J, Soerjomataram I et al: Global cancer statistics 2018: GLOBOCAN estimates of incidence and mortality worldwide for 36 cancers in 185 countries. Cancer J Clin, 2018; 68(6): 394–424
2. Yang X, Ye X, Lin Z et al: Computed tomography-guided percutaneous microwave ablation for treatment of peripheral ground-glass opacity-Lung adenocarcinoma: A pilot study. J Cancer Res Ther, 2018; 14(4): 764–71
3. Narsule CK, Sridhar P, Nair D et al: Percutaneous thermal ablation for stage IA non-small cell lung cancer: long-term follow-up. J Thorac Dis, 2017; 9(10): 4039–45
4. Yang X, Ye X, Zhang L et al: Microwave ablation for lung cancer patients with a single lung: Clinical evaluation of 11 cases. Thorac Cancer, 2018; 9(5): 548–54
5. Sidoff L, Dupuy DE: Clinical experiences with microwave thermal ablation of lung malignancies. Int J Hyperthermia, 2017; 33(1): 25–33
6. Vogl TJ, Nour-Eldin NA, Albrecht MH et al: Thermal ablation of lung tumors: focus on microwave ablation. Rofo, 2017; 189(9): 828–43
7. de Baere T, Tselikas L, Catena V et al: Percutaneous thermal ablation of primary lung cancer. Diagn Interv Imaging, 2016; 97(10): 1019–24
8. David A, Ray A, Hermet PL et al: Reduction of metallic coil artifacts in CT angiography with metal artefact reduction (MAR) algorithm. Diagn Interv Imaging, 2019; 100(6): 381–82
9. Peng C, Qiu B, Li M et al: Gaussian diffusion sinogram inpainting for X-ray CT metal artifact reduction. Biomed Eng Online, 2017; 16(1): 1
10. Wellenberg RHH, Hakvoort ET, Slump CH et al: Metal artifact reduction techniques in musculoskeletal CT-imaging. Eur J Radiol, 2018; 107: 60–69
11. Dong Y, Shi AJ, Wu JL et al: Metal artifact reduction using virtual monochromatic images for patients with pedicle screws implants on CT. Eur Spine J, 2016; 25(6): 1754–63
12. Hu Y, Pan S, Zhao X et al: Value and clinical application of orthopedic metal artifact reduction algorithm in CT scans after orthopedic metal implantation. Korean J Radiol ,2017; 18(3): 526–35
13. Wang F, Zhang Y, Xue H al: Combined use of iterative reconstruction and monochromatic imaging in spinal fusion CT images. Acta Radiol, 2017; 58(1): 62–69
14. Sekir U, Yildiz Y, Hazneci B et al: Reliability of a functional test battery evaluating functionality, proprioception, and strength in recreational athletes with functional ankle instability. Eur J Phys Rehabil Med, 2008; 44(4): 407–15
15. Yao W, Lu M, Fan W et al: Comparison between microwave ablation and lobectomy for stage I non-small cell lung cancer: A propensity score analysis. Int J Hyperthermia, 2018; 34(8): 1329–36
16. Zhong L, Sun S, Shi J et al: Clinical analysis on 113 patients with lung cancer treated by percutaneous CT-guided microwave ablation. J Thorac Dis, 2017; 9(3): 590–97
17. Das M, Abdelmaksoud MH, Loo BW Jr., Kothary N: Alternatives to surgery for early stage non-small cell lung cancer-ready for prime time? Curr Treat Options Oncol, 2010; 11(1–2): 24–35
18. Yang X, Ye X, Zheng A et al: Percutaneous microwave ablation of stage I medically inoperable non-small cell lung cancer: Clinical evaluation of 47 cases. J Surg Oncol, 2014; 110(6): 758–63
19. Kurilova I, Gonzalez-Aguirre A, Beets-Tan RG et al: Microwave ablation in the management of colorectal cancer pulmonary metastases. Cardiovasc Intervent Radiol, 2018; 41(10): 1530–44
20. Ni X, Han JQ, Ye X, Wei ZG: Percutaneous CT-guided microwave ablation as maintenance after first-line treatment for patients with advanced NSCLC. Onco Targets Ther, 2015; 8: 3227–35
21. Aissa J, Boos J, Sawicki LM et al: Iterative metal artefact reduction (MAR) in postsurgical chest CT: Comparison of three iMAR-algorithms. Br J Radiol, 2017; 90(1079): 20160778
22. Huang JY, Kerns JR, Nute JL et al: An evaluation of three commercially available metal artifact reduction methods for CT imaging. Phys Med Biol, 2015; 60(3): 1047–67
23. Andersson KM, Nowik P, Persliden J et al: Metal artefact reduction in CT imaging of hip prostheses-an evaluation of commercial techniques provided by four vendors. Br J Radiol, 2015; 88(1052): 20140473
24. Lee YH, Park KK, Song HT et al: Metal artefact reduction in gemstone spectral imaging dual-energy CT with and without metal artefact reduction software. Eur Radiol, 2012; 22(6): 1331–40
25. Diehn FE, Michalak GJ, DeLone DR et al: CT dental artifact: Comparison of an iterative metal artifact reduction technique with weighted filtered backprojection. Acta Radiol Open, 2017; 6(11): 2058460117743279
26. Park J, Kim SH, Han JK: Combined application of virtual monoenergetic high keV images and the orthopedic metal artifact reduction algorithm (O-MAR): Effect on image quality. Abdom Radiol (NY), 2019; 44(2): 756–65
27. Sunwoo L, Park SW, Rhim JH et al: Metal artifact reduction for orthopedic implants: Brain CT angiography in patients with intracranial metallic implants. J Korean Med Sci, 2018; 33(21): e158
28. Ragusi M, van der Meer RW, Joemai RMS et al: Evaluation of CT angiography image quality acquired with single-energy metal artifact reduction (SEMAR) algorithm in patients after complex endovascular aortic repair. Cardiovasc Intervent Radiol, 2018; 41(2): 323–29

Indexed in: [Current Contents/Clinical Medicine] [SCI Expanded] [ISI Alerting System] [ISI Journals Master List] [Index Medicus/MEDLINE] [EMBASE/Excerpta Medica] [Chemical Abstracts/CAS]

29. Magarelli N, De Santis V, Marziali G et al: Application and advantages of monoenergetic reconstruction images for the reduction of metallic artifacts using dual-energy CT in knee and hip prostheses. Radiol Med, 2018; 123(8): 593–600
30. Laukamp KR, Lennartz S, Neuhaus VF et al: CT metal artifacts in patients with total hip replacements: for artifact reduction monoenergetic reconstructions and post-processing algorithms are both efficient but not similar. Eur Radiol, 2018; 28(11): 4524–33
31. Yue D, Fan Rong C, Ning C et al: Reduction of metal artifacts from unilateral hip arthroplasty on dual-energy CT with metal artifact reduction software. Acta Radiol, 2018; 59(7): 853–60
32. Grosse Hokamp N, Laukamp KR, Lennartz S et al: Artifact reduction from dental implants using virtual monoenergetic reconstructions from novel spectral detector CT. Eur J Radiol, 2018; 104: 136–42
33. Shen ZL, Xia P, Klahr P, Djemil T: Dosimetric impact of orthopedic metal artifact reduction (O-MAR) on Spine SBRT patients. J Appl Clin Med Phys, 2015; 16(5): 106–16

Indexed in: [Current Contents/Clinical Medicine] [SCI Expanded] [ISI Alerting System] [ISI Journals Master List] [Index Medicus/MEDLINE] [EMBASE/Excerpta Medica] [Chemical Abstracts/CAS]